Physics of Plasmas

Positive corona streamer interaction with metalized dielectric: Possible mechanism of cathode destruction

Cite as: Phys. Plasmas **29**, 064501 (2022); https://doi.org/10.1063/5.0093203
Submitted: 27 March 2022 • Accepted: 20 May 2022 • Published Online: 02 June 2022

O. Emelyanov, A. Plotnikov and E. Feklistov

Physics of Plasmas BRIEF COMMUNICATION scitation.org/journal/php

Positive corona streamer interaction with metalized dielectric: Possible mechanism of cathode destruction

Cite as: Phys. Plasmas **29**, 064501 (2022); doi: 10.1063/5.0093203
Submitted: 27 March 2022 · Accepted: 20 May 2022 ·
Published Online: 2 June 2022

O. Emelyanov,[a] A. Plotnikov, and E. Feklistov

AFFILIATIONS

Peter the Great St. Petersburg Polytechnic University, 195251 St. Petersburg, Russia

[a]Author to whom correspondence should be addressed: oaemel2@gmail.com

ABSTRACT

This paper examines the effect of pulsed positive point-to-plane corona discharge in millimeter air gaps on the surface of a metalized dielectric. A footprint method was applied to reveal the streamer–surface interaction with Al and Zn thin films (20–50 nm) as a sensitive indicator. A thin metal film-dielectric substrate system was destructed at relatively low typical average currents of 20–50 μA during exposure times of 2–200 s. Destruction occurred in local zones with a size of several μm^2 per one discharge pulse, which is substantially lower than the conventional streamer size of several tens of micrometers. An offered model of electro-thermal heating of the cathode layer shows that the dielectric surface temperature can achieve 1000 K and more during the single current pulse of submicrosecond duration. The indicated mechanism is possibly responsible for the effects of the discharge plasma interaction with low heat conductivity cathodes, including biological objects. Intensive heating of the cathode layer should be considered when modeling the streamer–cathode interaction.

In the past few decades, intensive research has been conducted on the use of nonequilibrium cold atmospheric pressure plasma (CAP) in various fields. One of the most convenient forms of CAP formation is corona discharge (CD), which is used in numerous engineering applications such as ozone production,[1,2] reduction of gaseous pollutants (pollution control),[3] and surface treatment.[4] Corona discharge-produced ionic wind has drawn considerable attention from researchers for solving the thermal problems originating from the heat accumulation in small-scale devices.[5] The high chemical activity and limited thermal damage (average volume temperature $<45\,^{\circ}$C) of the CAP enable the use of plasma to act directly on biological objects.[6] The effect of gas discharge plasma on biological cells and living tissues is usually associated with reactive oxygen and nitrogen species (RONS),[7] ultraviolet radiation, electric field, and discharge current. It has now been proven that CD can effectively be used for the inactivation of various bacteria, viruses, and other pathogenic factors as well as plasma wound healing.[8–12]

It is generally accepted that the positive pulsed streamer CD effects are not related to thermal action since, in the classical representation, the overheating of the streamer channel is 5–10 K,[13] which is easy to show for the streamer channel radius R_s of the order of 0.5–1 mm. Meanwhile, the R_s can be much smaller for mm's gaps. In early works, the characteristic size of the streamer channel was estimated at 10–40 μm,[14,15] which is lower than the typical size values for streamers under the conditions of relatively long air gaps investigated in Refs. 16–18. The streamer channel radius R_s in mm gaps can be much less than 100 μm, which was recently shown in Ref. 19, where the discharge was an accumulation of about 100 or more channels with a size of $R_s \sim 0.1$–10 μm. Using streamer temperature evaluation models (e.g., in Ref. 13), and assuming R_s of ~0.1 mm, one can obtain an estimate of the overheating at the level of 200–300 K. Due to the process of nonequilibrium vibrational kinetics, the fraction of electron energy η transferred to heat is assumed in some works at $\eta \sim 0.3$–0.5, which is in good agreement with the experimental data.[20] Analysis of the observations in a high reduced electric field of $E/N = 10^3$ Td demonstrates a very high estimated value $\eta \sim 45\%$–65% on an extremely short time scale $pt \sim 1$ μs·atm.[21–23] As soon as the streamer bridges the gap, a cathode-fall region of high electric field and high positive-ion densities is established in the abnormal form of a glow discharge with the cathode fall of 600–700 V and even much greater.[24] The cathode fall of the glow discharge just under the glow-spark (arc) transition at 1000 K is $U_c = 1.9$ kV.[25] To avoid a temperature increase, one can use a resistor limiting the discharge current[3,11] and/or use the pulsed mode in the submicrosecond time range (NRP, nanosecond

repetitively pulsed discharge). The streamer corona, single filament, transient glow, dc glow, and spark (arc) modes and their transitions were also investigated in Ref. 26.

In this brief communication, the CD parameters utilized in the present study were close to those widely used in various applications: average currents of 10–50 μA, operating voltages of 5–15 kV in 1–8 mm air gaps, current pulse amplitudes of 10–50 mA, and a repetition rate of 10–30 kHz. Exposure times were in the range of tens and hundred seconds, which are typical for CD surface treatment applications.

The experiments were conducted in a laboratory facility, where the relative humidity was maintained between 30% and 40%. A footprint method and electric characteristic measurements were used to investigate streamer–cathode surface interaction (see Fig. 1). Thin aluminum and zinc metal films of thicknesses $\delta_m = 20$–50 nm coated on the dielectric substrate served as a cathode. A pin anode with the diameter of 0.8 mm and the tip curvature radius of about 40 μm was used. A high potential was applied to the pin anode from the DC high voltage (HV) supply through the current-limiting resistor $R_{ext} = 33$ MΩ. Prepared samples were mounted on the gas discharge cylindrical chamber (height 5 cm, volume 62 cm^3), wherein the metalized side faced the needle, and the substrate side faced the outside of the chamber. In order to diminish the oxidation and to study the thermal effect of the streamer–cathode interaction, the discharge chamber was mounted with inlet and outlet openings (pumping rate 2.0 l/min). This, in turn, ensured the renewal of the gas-discharge medium every second. The chamber was installed onto the base of the optical microscope, providing *in situ* observations of the cathode destruction. The streamer footprints were observed through an optical microscope in transmitted light mode (TLM), with magnification up to 1000× using a 5 MP digital camera. The morphology analysis of the samples treated by the discharge was additionally performed using the JEOL JSM-7001F Schottky Emission Scanning Electron Microscope (SEM, high resolution of 2 nm). Current pulses were measured with a low-inductive current shunt, $R_{pr} = 43$ Ω. A special divider with a capacitive loop 0.3 pF was developed that ensured the minimum effect of the measuring circuit on the gas-discharge process. Both current and voltage signals were transmitted to the inputs of the digital oscilloscope (Rohde & Schwarz RTB2004 2.5 Gs/s), providing measurements of rapidly changing processes. Figure 1 shows the integral photograph of the discharge development. It can be seen that the streamers develop from the positive needle electrode and propagate toward the cathode surface. There, they form cathode spots for a very short time, leading to thin metal film destruction (Fig. 1, demetalized area). The bright edge is due to the cathode spots forming for a very short time, leading to thin metal film

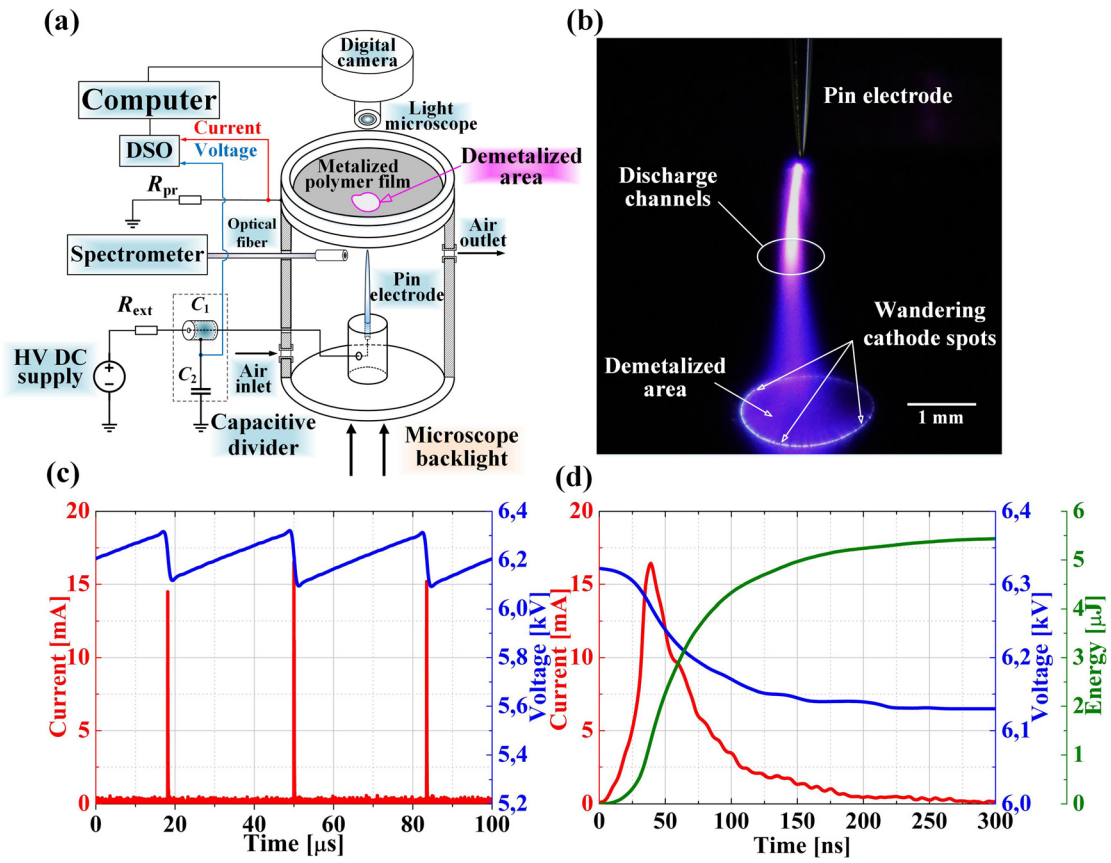

FIG. 1. Experimental setup (a), integral photograph of the corona discharge (b), typical current and voltage waveforms (c) and (d).

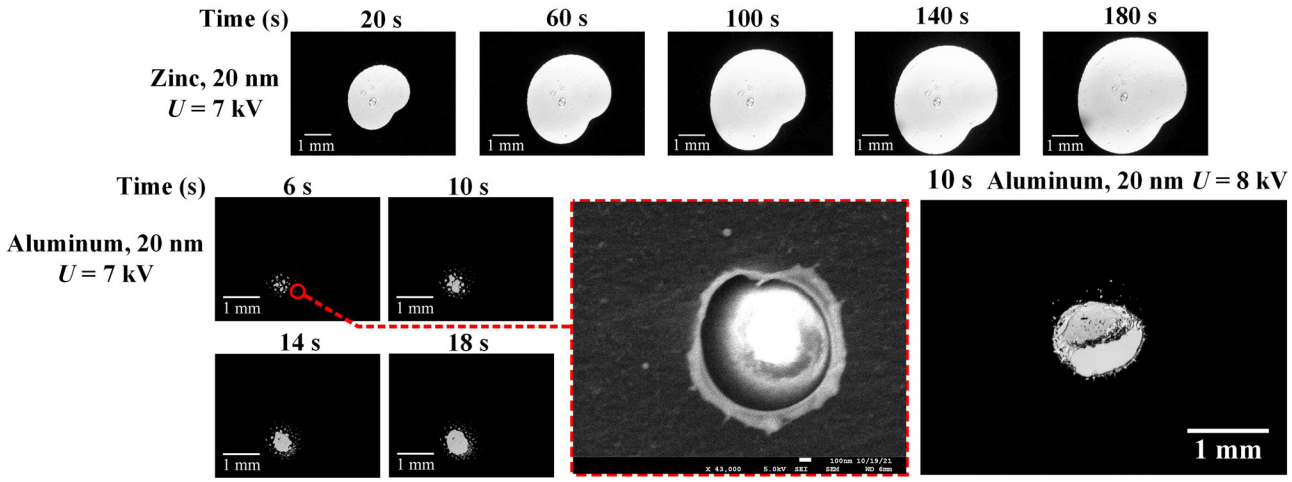

FIG. 2. TLM images of zinc and aluminum film destruction with a time exposure and SEM details. Melted polymer photograph is presented in the right bottom corner.

destruction. Thereafter, these spots merge into the main demetalized area, which grows almost symmetrically in the radial direction. The current and voltage waveforms are presented below (see Fig. 1). The typical discharge energy value was around units of microjoules and is depicted in Fig. 1. Figure 2 presents microphotographs of the destruction dynamics of aluminum and zinc films, where the black regions in TLM photographs represent intact metal. Observations demonstrated that the metal layer destruction begins with the appearance of demetallization zones having a typical size of several micrometers. Thereafter, these areas merge into the main demetalized spots, which grow almost symmetrically in the radial direction. In addition, the insignificant enhancing (~10%) of applied voltage can lead to polymer melting (see Fig. 2).

Considering the linearity of $\Delta S/\Delta\tau$ shown in Fig. 3, we get an average single destruction area $S_0 = 1.5$–$2\,\mu\text{m}^2$ for aluminum and $S_0 = 2$–$4\,\mu\text{m}^2$ for zinc (both for the metal layer thickness of 20 nm), which is significantly less than the area of the streamer head. These estimates are in good agreement with actually observed destruction areas captured using SEM. The small destruction zones can be explained by the rapid contraction of the discharge due to the development of instabilities during the intense heating of the cathode layer (CL). The contraction of a discharge in an atmospheric pressure plasma can be caused by thermal (ionization-overheating) instability, the effect of exothermic reactions and fast mechanisms of chemical heat release, electron attachment instability, electron maxwellization instability, etc. However, the complicated analysis of the development of instability is beyond the scope of the present brief communication. Hypothetically, electric explosion, cathode sputtering, chemical action, arc destruction, or heating of cathode layer influence can cause cathode destruction.

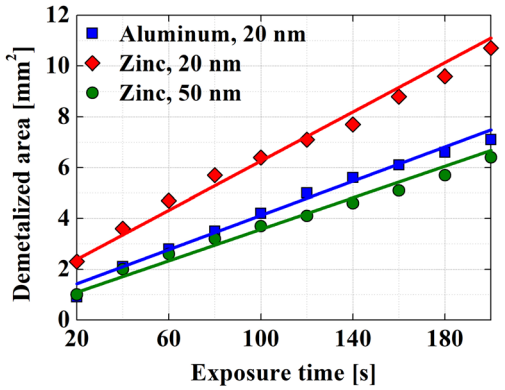

FIG. 3. Demetalized area dependence on exposure time.

First, assuming the discharge current pulse exponentially decaying function with amplitude I_m and a characteristic fall time of $\tau_{pul} \sim 100$ ns, the upper estimate of current specific action integral $\Im$ for the explosion time $\tau_{ex} \sim 400$–500 ns in the lateral surface of cathode spot with a radius even of $R_s \sim 1\,\mu$m, and a metal layer thickness δ_m can be expressed as follows:

$$\Im = \int_0^{\tau_{ex}} j^2 dt \approx \left[\frac{I_m}{2\pi R_s \delta_m}\right]^2 \frac{\tau_{pul}}{2} = 2 \cdot 10^{15},\ \text{A}^2/\text{m}^4\text{s}. \quad (1)$$

This is about two orders of magnitude lower than the value necessary for the electric explosion of an Al conductor $\sim 10^{17}$ A^2/m^4 s and for Zn is an order of magnitude lower.[27,28]

Second, the cathode sputtering of the metal cathode by ions is also unlikely. Generally, ions having energies of many keV are capable of sputtering metal electrode (cathode). In short gaps at atmospheric pressure,[29,30] these constants can differ from common values,[13] so that the cathode drop can reach 600–700 V and the layer thickness is about 20 μm at atmospheric pressure of 760 Torr. These estimates are close to the results of Ref. 18, where the reduced field E/N was approximately 1300–1400 Td, with a layer thickness of 20 μm. This, in turn, gives us an approximate ion energy of ~30 eV in the cathode fall. In addition, we estimated the sputtering yields of $Y \sim 0.2$–0.6, which are unreal values for the case of ion energies of a few tens of eV that are below the threshold of noticeable cathode sputtering.

Third, another way of metal destruction is due to oxidation (burning) of the metal film.[31] This process is relatively slow and, for instance, the Al burning time for our case can be expressed as $t_b \sim \rho_m (2\delta_m)^2/32DC_{ox,a}$, where $C_{ox,a}$ is the concentration of oxygen in the air and $D \sim 10^{-8}$ m^2/s is the oxygen diffusion coefficient. The estimation of t_b is of ~100 μs much more than the characteristic discharge time $\tau_{pul} \sim 100$ ns.

Fourth, another possible mechanism of the metal film-dielectric substrate system destruction is arcing. Under comparable conditions, it requires discharge pulse energy of the order of several hundred microjoules. However, in our case, the calculated W_{pul} values were 3–6 μJ (see Fig. 1) per pulse for all discharge modes, which rather corresponds to a glow NRP discharge mode or filamentary-transient glow discharge.[25,26] A transition of the corona into a glow discharge was considered in Ref. 32, where the characteristics of the spots did not correspond to standard arc discharge characteristics. This peculiar nature of the cathode spot is called the pre-arc cathode spot. Apparently, this type of spot is observed in our case. As shown by Hantzsche,[33] for an arc discharge duration of 10–100 ns, the average typical current density within the arc spot surface is expected to be 10^{12} A/m^2, and the power density more than 10^{12} W/m^2. Yet, the upper estimate of current density in our experiments yields only 10^{10} A/m^2, which is by far insufficient for arc spot formation. Moreover, computed erosion rates normalized by discharge energy are quite high and exceed those for atmospheric arcs by several orders: 0.2 μg/J for aluminum, 0.8 and 1 μg/J for zinc layers of thicknesses of 20 and 50 nm, respectively. This fact could be explained by considering that the erosion rates presented in the literature refer to bulk cathodes with high thermal conductivity. However, a detailed answer to the question of whether the arc mechanisms cause the unusual effectiveness of metal destruction requires additional research, which is by far out of the scope of our work.

In our model, we consider the heat removal to the substrate from the cathode at the end of the pulse. As a primary streamer approaches the cathode, a cathode layer forms at the surface, which can lead to a significant gas temperature increase near the cathode. Then, the heated gas gives its thermal energy to the cathode, and the latter, in turn, to the polymer/glass substrates through thermal conduction. At the level of ~1000 K, intensive heating of the substrate can lead to its significant thermal expansion or, even, the polymer boiling up explosively,[34] which leads to cathode destruction.

To a first approximation, we assume that the characteristic time of the single streamer action τ_{pul} is ~100 ns, which corresponds to the time scale of the discharge current pulse decay (see Fig. 1).[35] In our case, the thermal penetration depth into the polymer can be estimated by $\delta_p \sim (a_p\tau_{pul})^{0.5} \sim 0.1$ μm, where $a_p = \lambda_{PP}/(\rho_{PP}C_P)$ and $\lambda_{PP} = 0.2$ W/m K, $\rho_{PP} = 910$ kg/m^3, $C_P = 1920$ J/kg K are the thermal conductivity, density, and specific heat capacity of polypropylene, respectively. For a dielectric substrate, the thermal penetration depth δ_g is around 0.3 μm. Since $\delta_g \ll d_p = 6$ μm, this problem can be considered as the heating of a semi-infinite polymer body considering a thin metal layer at its boundary. The main heat flux to the thermal penetration zone comes from the zone of the CL $-$ q_c. It is only a part of the specific power dissipation η effectively heats the air in a characteristic time so that $q_c \sim \eta I_m U_c/\pi R_s^2$, where I_m is the discharge current magnitude, U_d and U_c are the gap and CL voltages, and R_s is the streamer radius. We can take some average value of the fraction of electron energy transferred to heat $\eta \sim 0.5$ (see above). Although the heating time of the metal film is very small $\tau_m = \delta_m^2/a_m \sim 0.5$ ns ($a_m \sim 10^{-4}$ m^2/s), the polymer is heated to a depth of several δ_m for the discharge pulse duration. Therefore, it is necessary to consider the presence of a metal film on the substrate surface, and the problem of the temperature dynamics should be considered in two related terms: metal (temperature T_m) and polymer (temperature T_p):

$$\begin{cases} (\rho C_p)_m \dfrac{\partial T_m}{\partial t} = \lambda_{lat}\ \dfrac{1}{r}\dfrac{\partial}{\partial r}\left(r\dfrac{\partial T_m}{\partial r}\right) + \dfrac{q_c}{\delta_m} - \dfrac{\lambda_{pp}}{\delta_m}\dfrac{\partial T_p}{\partial z}\bigg|_{z=0}, \\ (\rho C_p)_{pp}\dfrac{\partial T_p}{\partial t} = \lambda_{pp}\Delta T_p\,,\ \ T_m = T_m(r,t)\,,\ T_p = T_p\,(r,z,t), \end{cases} \tag{2}$$

where Δ is the Laplace operator, λ_{lat} is the lateral thermal conductivity of a nanometric film, t is the time, r and z are the radial and axis coordinates, respectively. At the first approximation, we neglect the thermophysical parameters' temperature dependencies of the metal film and substrate, since in the heat equations (2) a more significant role is played by the dynamics of the source temperature growth q_c due to fast Joule heating. Under conditions of such values of overheating, the radiation cooling mechanism (Stefan–Boltzmann law) in cold arc discharges is a small percentage of the total discharge energy.[13] In addition, for the characteristics during time τ_{pul}, the convective heat transfer mechanism can be neglected.

For an estimation of the temperature dynamic, one can assume that the heat diffusion in the metal film for the $\tau_{pul} \sim 100$ ns is much less than the R_s and $q_c(t) = I_m U_c/\pi R_s^2 \exp(-t/\tau_{pul})$, and we can consider the problem of temperature dynamic closed to the solution of Eqs. (2) for $r = 0$ along the z-axis. For the case, we have the exact solution in convolution form for the overheating temperature $\vartheta_m = T(t) - T_{amb}$ defined by

$$\vartheta_m(t) = \frac{q_c(0)}{(\rho C_p \delta)_m}\int_0^t \exp\left(-\frac{t-x}{\tau_{pul}}\right)\exp(a^2 x)\,\mathrm{erfc}\left(a\sqrt{x}\right)dx, \tag{3}$$

where $a = (\lambda\rho C_p)_{PP}{}^{0.5}/(\rho C_p \delta)_m$. For the case under consideration ($U_c = 600$ V, $I_m = 16$ mA, $\eta = 0.5$, which are reasonable parameters of CD one could find in the literature), the temperature dynamics for several reasonable streamer diameters D_s is shown in Fig. 4. The maximum temperature value is observed at times of $\tau_{pul} \sim 100$ ns. For the streamer diameter of less than ~40 μm, the temperature can reach up to 1000 K and more.

The dependences of the discharge current magnitude on the pulse duration, corresponding to the melting points of aluminum (933 K) and zinc (693 K), are shown in Fig. 5.

The variation of the typical experimental parameters of the CD corresponds to the shaded area. The presented results indicate significant heating of the cathode during a single discharge, which can cause its destruction. However, the estimates obtained should rather be interpreted as a preparation for the subsequent stage of destruction associated with the contraction of the discharge into a small cathode spot. The results of the study have shown that the metal film-dielectric substrate system can be destructed under the action of pulsed positive CD with parameters widely used in various applications.

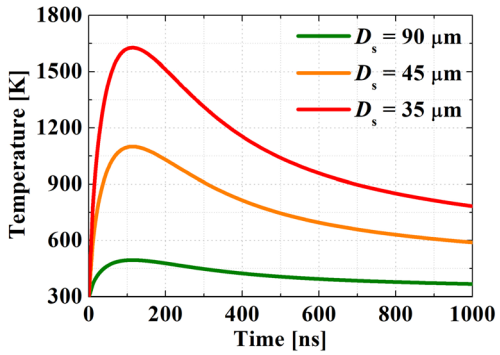

FIG. 4. Surface temperature dynamics for several streamer diameters.

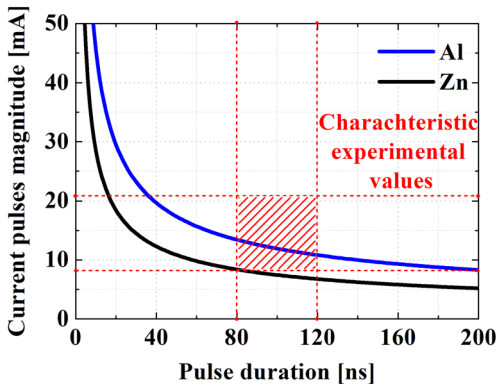

FIG. 5. Critical current magnitude dependencies on pulse duration corresponding to melting temperatures of Al and Zn.

We consider the heating of the cathode as a preparation for the subsequent stage of destruction associated with the rapid contraction of the discharge into a small cathode spot due to the development of plasma instabilities. The complicated analysis of the development of the instability is beyond the scope of the present paper.

It is generally believed that the disinfection and sterilization effects of cold plasma are mainly due to reactive oxygen species and reactive nitrogen species, and the thermal impact is very weak. This is true for indirect cold plasma sources, e.g., plasma-jets. Meanwhile, under the action of the direct cold plasma, the thermal effects are important to consider. For instance, the treated surface temperature increase is observed in the case of the filamentary dielectric barrier discharge,[35] with filaments characteristics closed to observed in our experiments. The found thermal effect of the streamer–cathode interaction probably can significantly affect the direct plasma sterilization. However, this requires more experimental studies on biological objects. Furthermore, for clarifying the physics of streamer–surface interaction, we are planning to investigate the corona discharge action in Ar and He, eliminating the effect of oxidation in air.

See the supplementary material for the video file demonstrating thin-film cathode destruction kinetics during exposure time of 20 s.

This work was supported by the Russian Science Foundation under Project No. 19-79-10075.

AUTHOR DECLARATIONS

Conflict of Interest

The authors have no conflicts to disclose.

DATA AVAILABILITY

The data that support the findings of this study are available from the corresponding author upon reasonable request.

REFERENCES

[1]J. Chen and J. H. Davidson, Plasma Chem. Plasma Process. **22**, 495–522 (2002).
[2]A. Yehia, J. Appl. Phys. **101**, 023306 (2007).
[3]O. Eichwald, O. Ducasse, D. Dubois, A. Abahazem, N. Merbahi, M. Benhenni, and M. Yousfi, J. Phys. D **41**, 234002 (2008).
[4]M. Stepczyńska and M. Zenkiewicz, Polimery **59**, 220–226 (2014).
[5]J. Wang, T. Zhu, Y. Cai, J. Zhang, and J. Wang, Int. J. Heat Mass Transfer **152**, 119545 (2020).
[6]A. Fridman and G. Fridman, *Plasma Medicine* (John Wiley and Sons, 2013), pp. 1–35.
[7]X. Lu, G. V. Naidis, M. Laroussi, S. Reuter, D. B. Graves, and K. Ostrikov, Phys. Rep. **630**, 1–84 (2016).
[8]D. Dobrynin, G. Friedman, A. Fridman, and A. Starikovskiy, New J. Phys. **13**, 103033 (2011).
[9]E. Sysolyatina, A. Mukhachev, M. Yurova, M. Grushin, V. Karalnik, A. Petryakov, N. Trushkin, S. Ermolaeva, and Y. Akishev, Plasma Process. Polym. **11**, 315–334 (2014).
[10]T. Liu, Y. Zeng, J. Chen, D. Wei, Q. Zeng, Y. Fu, Y. Fu, F. Yang, and F. Feng, IEEE Trans. Plasma Sci. **49**, 317–325 (2021).
[11]O. A. Emelyanov, E. G. Feklistov, N. V. Smirnova, K. A. Kolbe, E. V. Zinoviev, M. S. Asadulaev, A. A. Popov, A. S. Shabunin, and K. F. Osmanov, AIP Conf. Proc. **2179**, 20006 (2019).
[12]O. A. Emelyanov, N. O. Petrova, N. V. Smirnova, and M. V. Shemet, Tech. Phys. Lett. **43**, 742–744 (2017).
[13]Y. P. Raizer, in *Gas Discharge Physics*, edited by J. E. Allen (Springer, Berlin, Heidelberg, 1991).
[14]E. Marode, F. Bastien, and M. Bakker, J. Appl. Phys. **50**, 140–146 (1979).
[15]M. Goldman, A. Goldman, and R. S. Sigmond, Pure Appl. Chem. **57**, 1353–1362 (1985).
[16]S. Pancheshnyi, M. Nudnova, and A. Starikovskii, Phys. Rev. E **71**, 16407 (2005).
[17]A. Luque, V. Ratushnaya, and U. Ebert, J. Phys. D **41**, 234005 (2008).
[18]R. Ono and A. Komuro, J. Phys. D **53**, 35202 (2020).
[19]K. I. Almazova, A. N. Belonogov, V. V. Borovkov, Z. R. Khalikova, G. B. Ragimkhanov, D. V. Tereshonok, and A. A. Trenkin, Plasma Sources Sci. Technol. **30**, 95020 (2021).
[20]A. S. Petrusev, S. T. Surzhikov, and J. J. S. Shang, High Temp. **44**, 804–813 (2006).
[21]N. A. Popov, Plasma Phys. Rep. **27**, 886–896 (2001).
[22]N. L. Aleksandrov, S. V. Kindysheva, M. M. Nudnova, and A. Y. Starikovskiy, J. Phys. D **43**, 255201 (2010).
[23]N. A. Popov, J. Phys. D **44**, 285201 (2011).
[24]E. P. Velikhov, V. S. Golubev, and S. V. Pashkin, Sov. Phys.-Usp. **25**, 340–358 (1982).
[25]D. Z. Pai, D. A. Lacoste, and C. O. Laux, J. Appl. Phys. **107**, 93303 (2010).
[26]S. Wu, W. Cheng, G. Huang, F. Wu, C. Liu, X. Liu, C. Zhang, and X. Lu, Phys. Plasmas **25**, 123507 (2018).
[27]V. O. Belko and O. A. Emelyanov, J. Appl. Phys. **119**, 024509 (2016).
[28]V. O. Belko, O. A. Emelyanov, I. O. Ivanov, A. P. Plotnikov, and E. G. Feklistov, IEEE Access **9**, 80945–80952 (2021).
[29]V. R. Soloviev, J. Phys. D **45**, 25205 (2012).

[30]P. N. Bondarenko, O. A. Emelyanov, and M. V. Shemet, Tech. Phys. **59**, 838–846 (2014).
[31]D. S. Sundaram, V. Yang, and V. E. Zarko, Combust., Explos. Shock Waves **51**, 173–196 (2015).
[32]Y. Akishev, V. Karalnik, I. Kochetov, A. Napartovich, and N. Trushkin, Plasma Sources Sci. Technol. **23**, 54013 (2014).
[33]E. Hantzsche, IEEE Trans. Plasma Sci. **31**, 799–808 (2003).
[34]S. E. Puchinskis and P. V. Skripov, Int. J. Thermophys. **22**, 1755–1768 (2001).
[35]S.-Y. Kim, T. Lho, and K.-S. Chung, Phys. Plasmas **25**, 64503 (2018).
[36]H. Ayan, G. Fridman, D. Staack, A. Gutsol, V. Vasilets, A. Fridman, and G. Friedman, IEEE Trans. Plasma Sci. **37**, 113–120 (2009).